Influence of geometric imperfections on tapered roller bearings life and performance

Rodríguez R [a], Calvo S [a], Nadal I [b] and Santo Domingo S [c]

a Computational Simulation Centre, Instituto Tecnológico de Aragón, 7-8 María de Luna, 50018 Zaragoza, Spain.

b Design of Mechatronic Product Centre, Instituto Tecnológico de Aragón, 7-8 María de Luna, 50018 Zaragoza, Spain.

c R&D Department, FERSA Bearings S.A, 18 Bari, 50197 Zaragoza, Spain

Keywords: Tapered roller bearings, life prediction, contact pressure, misalignment, surface profile.

Performance and life in tapered roller bearing is highly influenced by contact pressure distribution in the raceways which is also determined by the contact area and profile geometry of the bearing components (rollers and rings). This complex geometry together with non-Hertzian effects (local yielding, edge effects…) makes impossible a precise analytical calculation of the contact pressure distribution. This contact distribution is evaluated instead by numerical calculations using virtual prototyping techniques (i.e: the finite element method). The use of finite element procedures allows the inclusion on the life calculations of imperfections in the profile finishing as well as misalignment in the axle mounting and angle errors on the raceways. The influence of these effects in the bearing performance has been analysed by using dynamic explicit simulations in terms of rolling torque and vibration. The results obtained from the finite element simulations have been validated and correlated with experimental results from a bearing test rig developed for this purpose. Thus, the use of virtual prototyping allows the prediction of bearings life, performance under adverse conditions and choice of profile combinations according to expected working conditions with a substantial reduction in time and costs.

1 Introduction

In the present paper, the influence of geometric imperfections (focusing in misalignment) on roller bearings life and performance is analysed by means of finite element calculations. The necessity of using finite element calculations will be stated by comparison with the results from theoretical formulas [1] due to the complex profile and non-Hertzian effects in the contacts. Next the finite element methodology developed is used to estimate the variation in the bearing life due to misalignment by using the highly extended empirical formulas [2] where the fatigue load limit is the parameter influenced by the misalignment. Finally, the influence of the misalignment on the rolling torque and friction is studied by dynamic finite element simulations.

2 Hertz contact theory and finite element approach

Hertz contact theory allows the calculation of contact characteristics between elastic curved bodies under certain hypothesis:

- The materials of the bodies in contact are homogeneous and isotropic.
- The materials yield stress is not surpassed, so plastic deformation can be neglected and only elastic deformation is considered.

- In the contact area only normal stress are transmitted. Shear stresses on the surface due to friction are not considered.
- Contact area is flat. Any curvature effect can be disregarded in a stress distribution analysis.

Accordingly, for contact between cylindrical bodies, the maximum pressure can be calculated:

$$p_{\max} = E_{eq}\left(\frac{\overline{W}}{2\pi}\right)^{1/2} \quad (1)$$

Where:

$$\overline{W} = \frac{W}{L \cdot E_{eq} \cdot R_x} \quad (2)$$

$$\frac{2}{E_{eq}} = \frac{1-\upsilon_1^2}{E_1} + \frac{1-\upsilon_2^2}{E_2} \quad (3)$$

$$\frac{1}{R_x} = \frac{1}{R_2} \pm \frac{1}{R_1} \quad (4)$$

In formula (4), the sign is positive for convex contacts and negative for concave contacts. In the previous formulas, E, R and υ are the elastic modulus, the equivalent contact radius and the Poison ratio of the bodies in contact.

Also, the contact width can be calculated:

$$a = 2R_x\left(\frac{8\overline{W}}{\pi}\right)^{1/2} \quad (5)$$

With only slight modifications, this methodology can be adapted to the tapered roller case, where the bodies in contact are not cylindrical but conical. This methodology has been compared with finite element calculations where a $1/2Z$ (being Z the number of rollers) section of a tapered roller bearing has been simulated (fig 1).

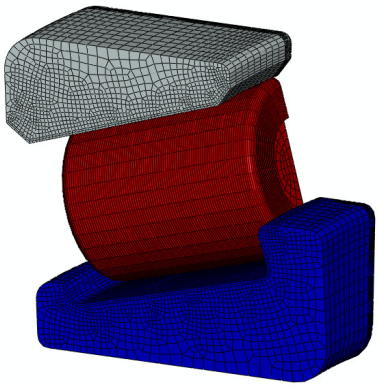

Fig 1 – Half-roller finite element model.

It was found out that although at the central zone of the contact area, the contact pressure distributions are quite similar, the Hertz formulas fail to reproduce the stress concentration due to edge effects at the longitudinal ends of the contact area. At the stress concentrations, the contact pressure increases in a 75%.

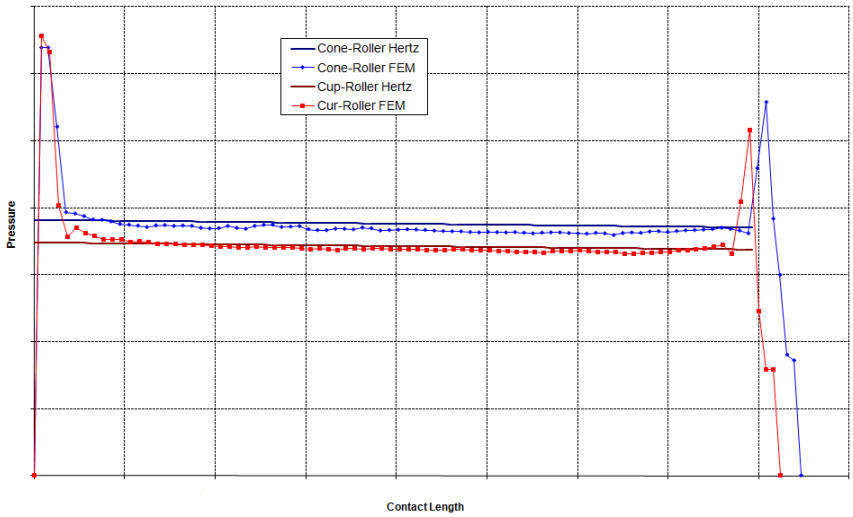

Fig 2 – Comparison of contact pressure distributions.

This stress concentrations are the main reason for the inclusion of complex profile geometry in the raceways, however, this stress concentration will appear with any profile if the load is risen high enough or if misalignment problems take place.

3 Rating life calculation

It is impossible to test every rolling bearing manufacturer reference at every combination of axial and radial load and velocity so it is widely extended the use of empirical formulas [2] as function of these parameters and other related to lubrication, contamination and fatigue.

Basically, these empirical formulas relate life with ratios between limit loads and equivalent operational loads. The procedure is summarized in formulas (6) to (8).

$$L = a_1 \cdot a_2 \cdot \left(\frac{C}{P}\right)^d \tag{6}$$

Where a_1 is a statistical parameter, C is the dynamic load rating of the bearing, P is the dynamic equivalent operational load and d is a parameter function of the bearing type. a_2 is a parameter function of lubrication, contamination and fatigue stress limit of the material.

$$a_2 = f\left(\kappa, e_c, \frac{\sigma_u}{\sigma}\right) \tag{7}$$

Where κ is a lubrication parameter, e_c a contamination parameter and σ_u and σ the fatigue stress limit, determined by the material quality, and the actual operational stress.
To facilitate practical calculation, a fatigue load limit (C_u) is introduced and the contamination factor coupled with the fatigue term.

$$a_2 = f\left(\kappa, e_c \frac{C_u}{P}\right) \tag{8}$$

Geometric imperfections, such as misalignment, mainly affect the value of the fatigue load limit. Although the fatigue stress limit does not change, the load at which that stress is reached changes relying on the geometric imperfections.

4 Finite element model for static simulations

Next, the finite element model is described.

Number of nodes	103613
Number of elements	91909

Tab 1 – Finite element model data.

The mesh has been refined at the contact zones (fig 3), with an average element size of 0.1mm. A surface to surface formulation has been used in both contact pairs with penalty enforcement method.

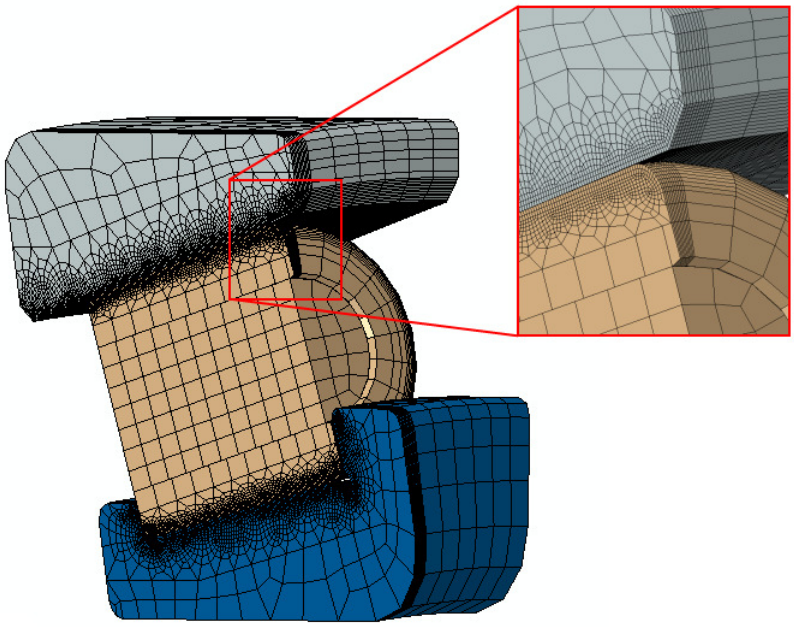

Fig 3 – Contact zone mesh detail.

In order to reduce computational costs of the model, the roller has been divided into two parts united by a tie constraint to avoid continuity in the refined zone of the mesh.

Symmetry boundary conditions have been applied to the vertical cutting plane (fig 4), also fully clamped boundary condition has been forced into the inner face of the cone (fig 5).

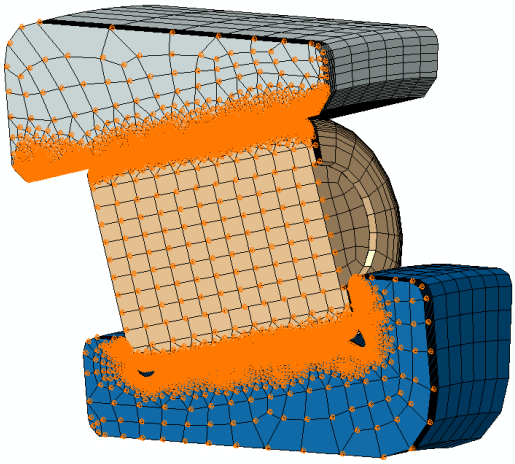

Fig 4 – Symmetry boundary conditions.

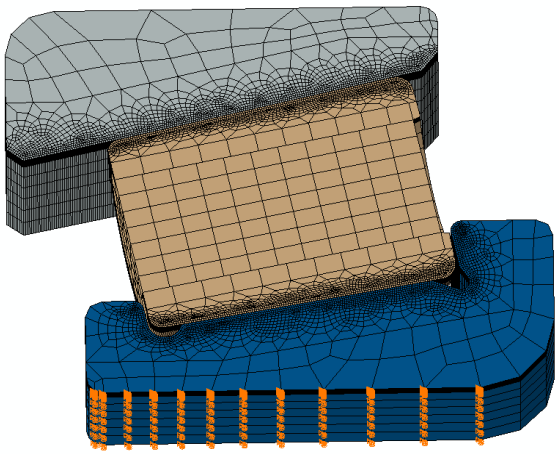

Fig 5 – Fully clamped boundary conditions.

Axial movement of the cup is restricted (fig 6). Load is applied radially on the cup outer face (fig 7) as a distributed load.

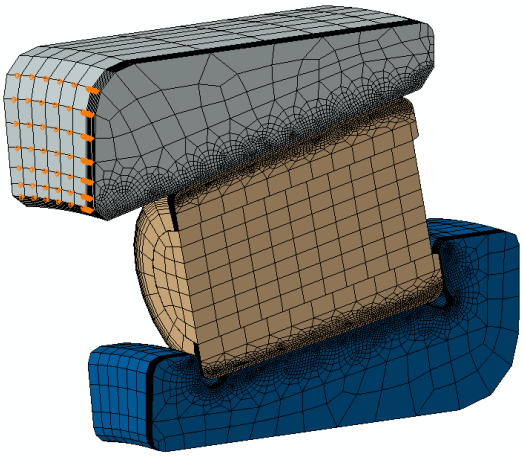

Fig 6 – Cup axial restriction.

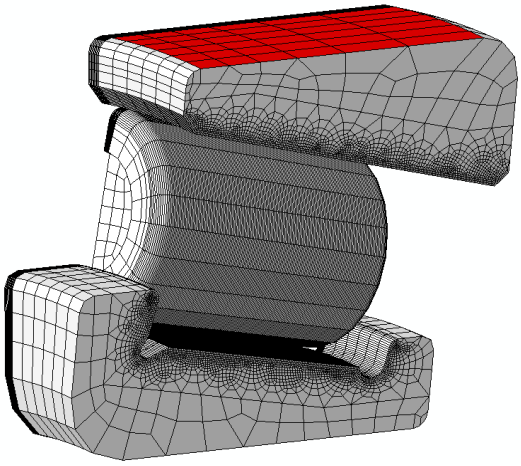

Fig 7 – Radial load.

5 Effect of misalignment on the rating life

In the previously described half-roller model, several misalignments have been included in the cone and the contact pressure distribution extracted at the theoretical contact line. At a given load, fig 8 shows the comparison of the contact pressure distribution for different misalignments.

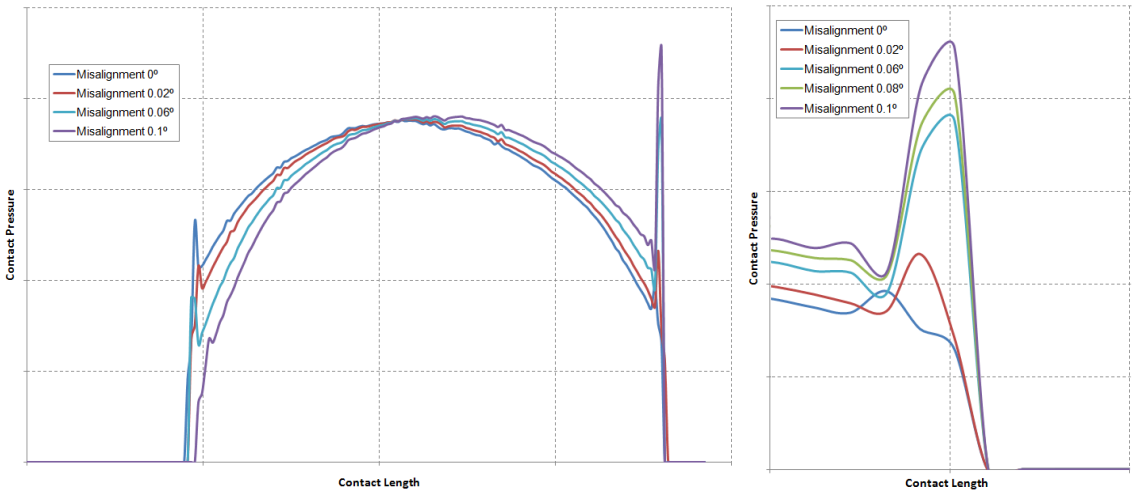

Fig 8 – Left, contact pressure distributions for different misalignment angles. Right, detail of the contact pressure concentration.

From a misalignment of 0.06º on, the contact pressure value at the edge concentration surpasses the maximum value at the centre zone of the contact area. Also, the central value of the contact pressure increases slightly with increasing misalignment.
From results at different load levels, a graphic displaying the fatigue load limit as a function of the fatigue stress limit can be constructed (fig 9).

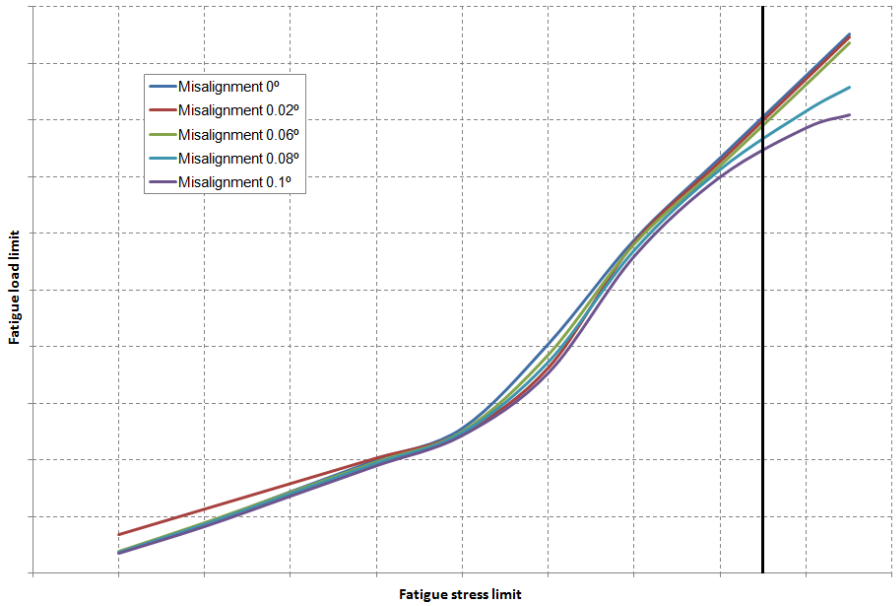

Fig 9 – Fatigue load limit versus fatigue stress limit for different misalignment angles.

It can be observed in fig 9 that for low-quality materials, the misalignment barely affects the fatigue load limit. However, for normal to high-quality materials (from the vertical line on), the fatigue load limit is reduced significantly. The reason is that at high load levels is when the concentration effects take place.

Tab 2 shows how the fatigue load limit and the rating life are reduced by effect of the misalignment for a given lubrication and load conditions.

	Fatigue load limit	Rating Life
Aligned	1.000	1.000
Misalignment 0.02º	0.994	0.994
Misalignment 0.06º	0.984	0.986
Misalignment 0.08º	0.967	0.971
Misalignment 0.1º	0.957	0.962

Tab 2 – Normalized fatigue load limit and normalized life.

The rating life is reduce fewer than the fatigue load limit due to the high non-linearity of the equations involved in the rating life calculation.

6 Finite element model for dynamic simulations

In order to carry out dynamic simulations, a full model of the tapered roller bearing is required (fig 10). The simulations consists of two parts, in the first the cone is accelerated up to the test velocity and in the second one the velocity is kept until the rolling torque is stabilized and enough points are obtained. Tab 3 shows the number of elements and nodes of the model.

Number of nodes	368271
Number of elements	230607

Tab 3 – Finite element model data.

Similarly to the static model, in order to reduce the computational cost of the model, a first layer of thin element has been used in the regions in contact (fig 11), in the cone as well as in the cup and rollers. Again, tie constraints have been used to join the superficial element with the rest of the part. It results in a minimum stable time increment of 1.579E-8s.

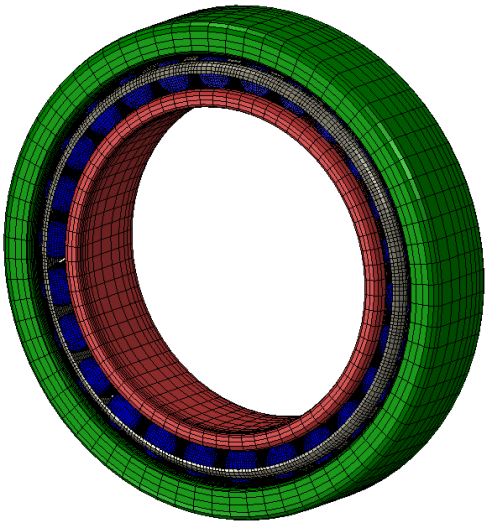

Fig 10 – Tapered roller bearing dynamic FE model.

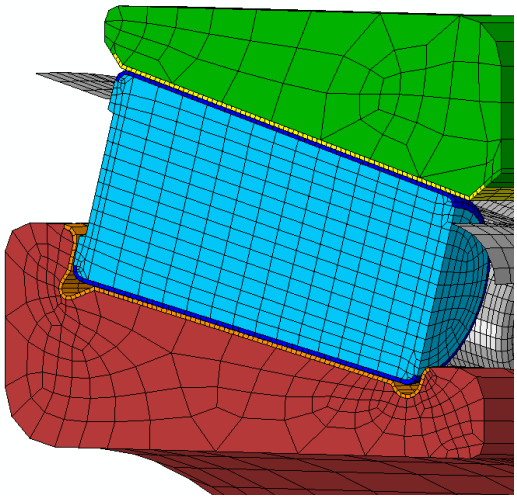

Fig 11 – Dynamic model mesh detail.

The outer nodes of the cup are clamped (fig 12). The inner nodes of the cone are kinematically coupled to a centered reference node, to which axial load and rotational velocity are applied (fig 13).

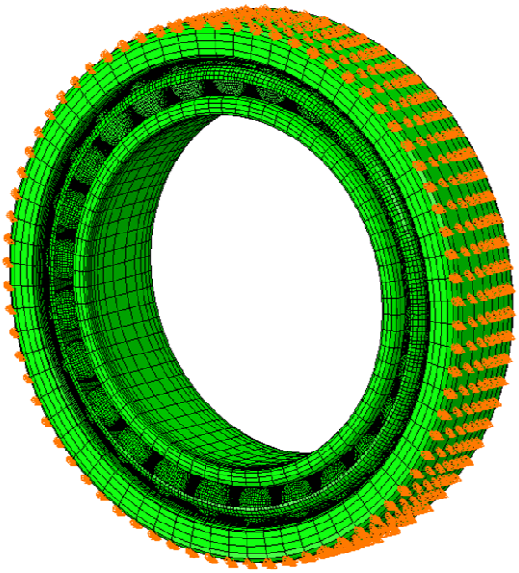

Fig 12 – Tapered roller bearing dynamic FE model.

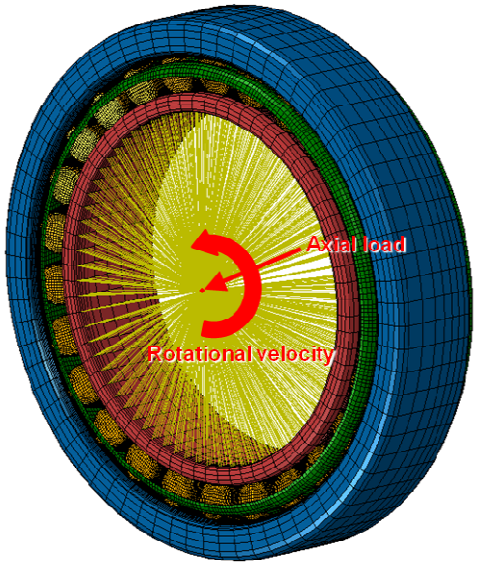

Fig 13 – Dynamic model mesh detail.

7 Effect of misalignment on the rolling torque

In the present section, the influence of the misalignment on the rolling torque and vibration characteristic is checked out. For this, several dynamic FE simulations have been carried out with the same conditions of load and velocity and different misalignment angles.

Due to the nature of the explicit dynamic finite element simulations, if accuracy in the contacts is required the stable time increment gets severely reduced, so only a brief span of time can be simulated.

Fig 11 shows the rolling torque obtained in a aligned and 0.06º misaligned tapered roller bearing. Time-history post-processing is not conclusive due to excessive noise in the signal. To avoid this problem, a FFT post-processing has been performed (fig 12).

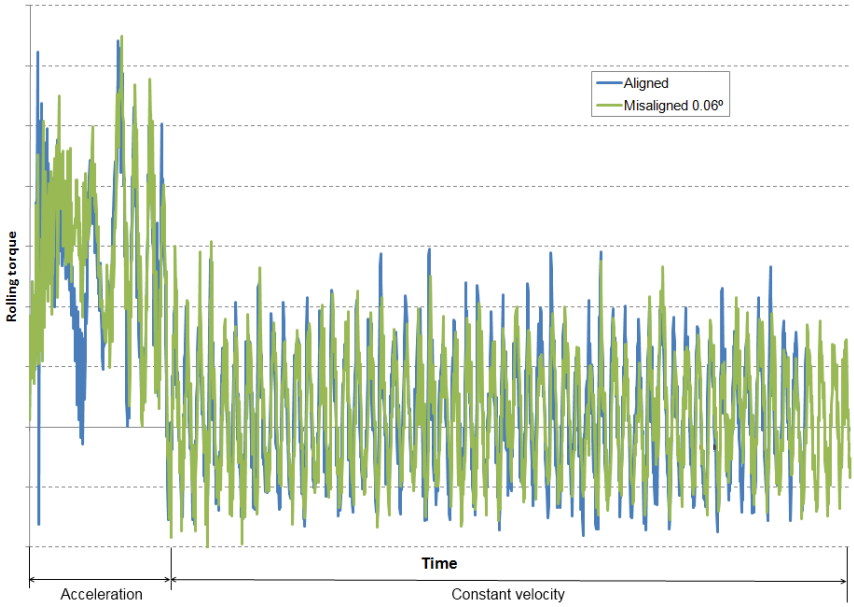

Fig 11 – Rolling torque over time from aligned and 0.06º misaligned tapered roller bearing.

In the Fast Fourier Transform of the rolling torque signals it can be observed that the peak caused by the discretization (at around 11 KHz), equivalent to shape defect in the rollers, is slightly reduced in the misaligned case, while peaks at lower frequencies increase.

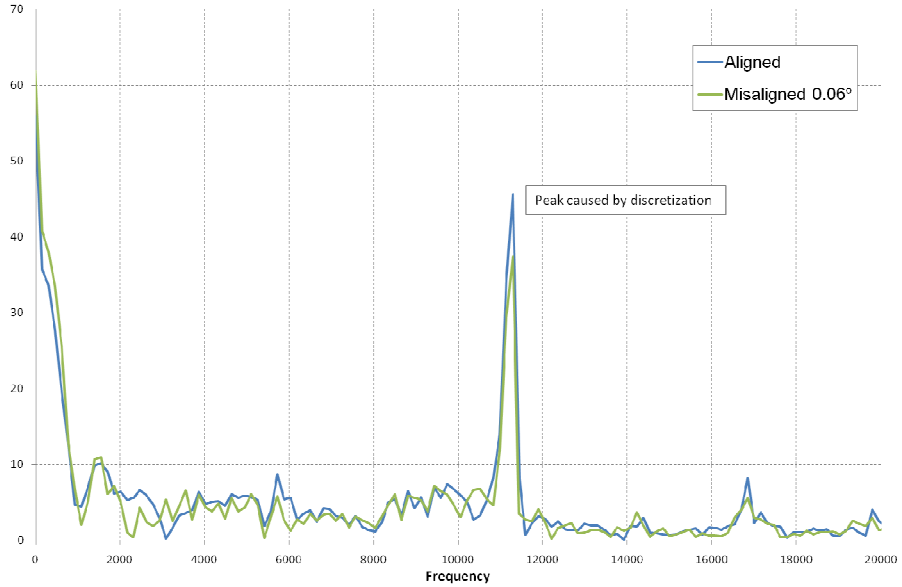

Fig 12 – FFT post-processing of the rolling torque signals.

The energy dissipated by friction in both simulations is gathered in fig 13. A higher amount of energy is dissipated in the acceleration part of the simulation in the misaligned case; also energy is dissipated by friction at a rate 7.3% higher in the misaligned case than in the aligned case in the stationary part of the simulation.

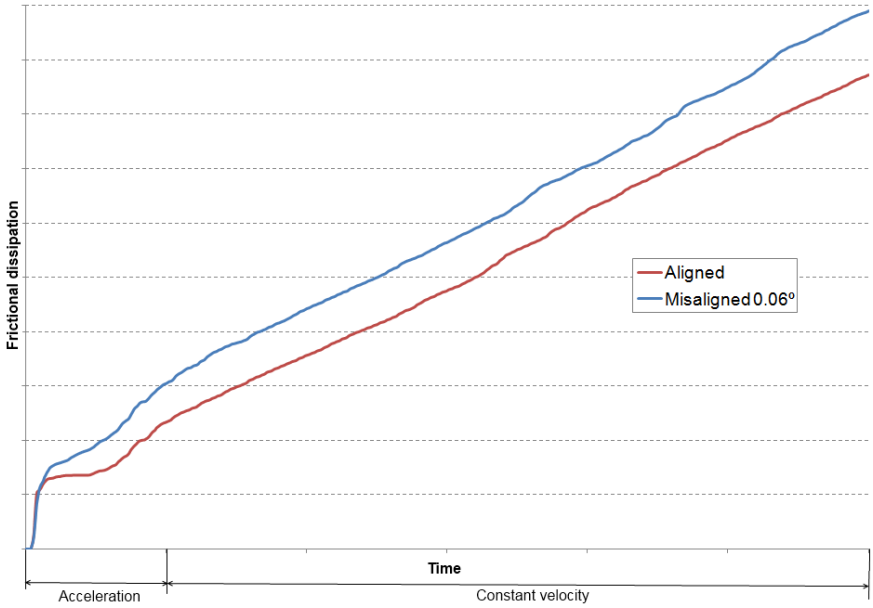

Fig 13 – Frictional dissipation from aligned and 0.06º misaligned tapered roller bearing.

8 Conclusions

The finite element method has been used in this paper to analyse the effect of misalignment on the rating life and rolling torque of tapered roller bearings. On the basis of the results obtained, the following conclusions can be drawn:

– The available theoretical contact formulas are not accurate enough for the problems encountered in tapered roller bearings due to the complex profiles of the bearing parts and the apparition of non-Hertzian effects at operational loads.
– These effects are taken into account by using finite element procedures.
– A misalignment in the tapered roller bearing reduces its rating life, but it is from a misalignment angle of 0.06º on when the life starts to reduce its value more radically, due to edge effects in the analysed case.
– This reduction takes place for normal to high-quality materials because the edge effects take place at high loads.
– Dinamically, the inclusion of a misalignment in a tapered roller bearing increases the rate of dissipation of energy in a 7.3% for a misalignment angle of 0.06º in the analysed case.

9 References

[1] Bearing Design in Machinery. Avraham Harnoy. Marcel Dekker, Inc.

[2] ISO 281:2007(E). Rolling bearings – Dynamic load ratings and rating life.

[3] Vibration characteristics of tapered roller bearings. H. Ohta and N.Sugimoto. Journal of Sound and Vibration (1996) 190(2), 137-147

[4] Rolling bearing analysis. Tedric A. Harris and Michael N. Kotzalas. CRC Press.